Stabilized fully-coupled finite elements for elastohydrodynamic lubrication problems

W. Habchi[1], D. Eyheramendy[2], P. Vergne[3] and G. Morales-Espejel[4]

[1] Lebanese American University (LAU), Department of Industrial and Mechanical Engineering, Byblos, Lebanon

[2] LMA, Ecole Centrale Marseille, CNRS UPR7051, 13451 Marseille Cedex 20, France

[3] Université de lyon, CNRS INSA-Lyon, LaMCoS, UMR 5259, F-69621, Villeurbanne, France

[4] SKF Engineering and Research Center, Nieuwegein, The Netherlands

Abstract:

This work presents a model for Elastohydrodynamic (EHD) lubrication problems. A finite element full-system approach is employed. The hydrodynamic and elastic problems are solved simultaneously which leads to fast convergence rates. The free boundary problem at the contact's exit is handled by a penalty method. For highly loaded contacts, the standard Galerkin solution of Reynolds equation exhibits an oscillatory behaviour. The use of artificial diffusion techniques is proposed to stabilize the solution. This approach is then extended to account for non-Newtonian lubricant behaviour and thermal effects. Artificial diffusion procedures are also introduced to stabilize the solution at high loads.

Keywords: Finite elements, Elastohydrodynamic lubrication, artificial diffusion, full-system approach.

1. Introduction

Nowadays, rolling element bearings are essential components in any mechanical system that includes rotating parts. This is because the direct contact between the rotating parts may damage them and lead to system failure. Moreover, direct contact leads to high frictional losses and a significant increase in the energy consumption of the system. Thus, bearings are introduced to prevent large surface metal-to-metal contact. In order to further improve the functioning of these components, they are lubricated. In other words, a lubricant (oil, grease, etc) is introduced between the contacting surfaces (rolling element and inner / outer raceway). It is therefore important for the good functioning of a bearing to have a reliable tool to estimate film thicknesses and frictional losses in the contact.

In this work, we are mainly interested in a particular lubrication regime known as Elastohydrodynamic (EHD). In this regime, the contacting bodies are separated by a full lubricant film. The pressure generated in the contact is high enough to induce a significant elastic deformation of the contacting bodies. Therefore, hydrodynamic and elastic effects are strongly coupled. When studying these contacts, it is not necessary to consider the often rather complex geometry of the contacting machine elements. Since the film thickness and contact width are generally small compared to the local radius of curvature of the running surfaces, the surface geometry in the contact area can be accurately approximated by paraboloids. This

approximation allows a simplification of the contact geometry. The latter can be reduced to the contact between a paraboloid and a flat surface. Two types of contacts may be distinguished: **line contacts** (See Figure 1) where the contacting elements are assumed to be infinitely long in one of the principal directions (e.g.: cylindrical roller bearings) or **point contacts** (See Figure 2) which occur between two parabolically shaped surfaces with local radii of curvature R_{1x} and R_{2x} in the x-direction and R_{1y} and R_{2y} in the y-direction. A special case of a point contact is the **circular contact** which occurs if the radii of curvature of the contacting elements in both principal directions are equal. This paper is mainly focused on the circular contact configuration. However, where needed, some line contact results are shown for demonstrative purposes.

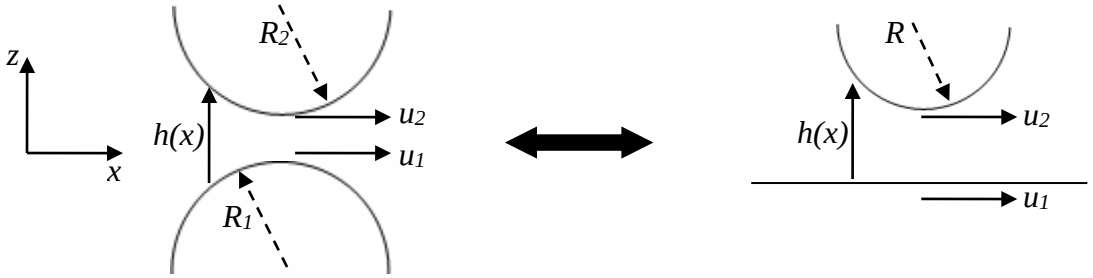

Figure 1: EHL line contact and the equivalent reduced geometry

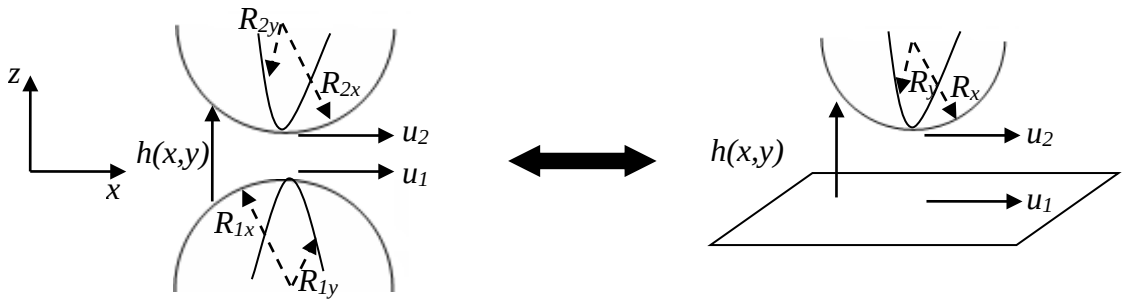

Figure 2: EHL point contact and the equivalent reduced geometry

In the past few decades, a large number of numerical solutions of the isothermal elastohydrodynamic lubrication (EHL) problem emerged. Most of these studies used a weak coupling resolution of the Reynolds (Hydrodynamic) and elasticity equations. The two equations were solved separately and an iterative procedure was applied between their corresponding solutions. A direct consequence of the weak coupling resolution is in general, a slow convergence rate of the global system. This can be partially explained by the use of underrelaxation techniques that are often necessary as a compensation to the loss of information that occurs during the iterative coupling process. Very few authors attempted to solve the fully coupled problem. Among them, we cite Oh and Rohde [1] who tried to solve the problem as one integro-differential equation using Newton's method, or also Holmes et al. [2] who used the differential deflection method to compute the elastic deformation of the contacting bodies. Although these attempts succeeded in finding a solution of the EHD problem with outstanding convergence rates (a few iterations were enough to obtain a converged solution), they suffered from three major drawbacks. First, because of the simultaneous solution of all pressure updates, the implementation of the cavitation condition at the outlet of the contact was rather tedious and second, the elastic deformation calculation was based on a half-space approach (Boussinesq solution). In this approach, the deformation at each point is related to pressure at all discretization points of the computational domain. This leads to a full Jacobian matrix. Despite some attempts to reduce the size of this matrix by

neglecting the smallest terms (e.g. see [2]), the computational effort and memory storage were still heavy. Finally, the Jacobian matrix was nearly singular for heavily loaded contacts which made the resolution process under such conditions particularly difficult. This is probably why this approach did not have as much success as the weakly coupled one, mostly based on a finite difference discretization of the corresponding equations and for which several efficient techniques were developed such as Multigrid techniques that were introduced to lubrication problems by Lubrecht [3] and further improved by Venner [4] who extended the solution to highly loaded contacts.

In an earlier work [5], the authors had already introduced a finite element approach to isothermal Newtonian EHL problems. The hydrodynamic and elastic problems were fully-coupled whereas an iterative procedure was established to ensure the load balance. The free boundary problem arising at the contact's exit was handled by a heavyside function. Later on, the authors extended this approach to account for non-Newtonian lubricant behaviour and thermal effects in lightly loaded contacts [6]. In this paper, a finite element fully-coupled resolution procedure is introduced. The load balance equation is integrated directly into the matrix system, providing thus a full-coupling of the three EHL equations (hydrodynamic, elastic and load balance equations). A penalty method is introduced to handle the free boundary problem in a straightforward manner. Appropriate stabilization techniques are applied to the Reynolds equation in order to extend the solution to highly loaded contacts. This approach has the advantage of providing a sparse Jacobian matrix, giving thus an efficient resolution of the fully-coupled problem with fast convergence rates. Then, this approach is extended to, first, non-Newtonian lubricants and second, thermal effects under light and heavy loads. In both cases, generalized forms of the Reynolds equation are considered.

2. Isothermal Newtonian approach

In this section, the lubricant is assumed to behave as a Newtonian fluid and thermal effects are neglected in the contact (temperature throughout the lubricant film is considered constant and equal to the ambient temperature T_0). The contacting surfaces are submitted to a prescribed external load F and have constant unidirectional surface velocities in the x-direction.

Mathematical model

This section presents the mathematical model used to describe the behaviour of EHD contacts under isothermal Newtonian regime. This model is the basis of the EHL solver presented in this work, from which, an extension to a more physical modelling can be carried out.

EHL theory and equations

Three main equations define an EHL problem: the Reynolds equation which describes the pressure distribution p in the contact area, the linear elasticity equations which determine the elastic deformation of the contacting elements and the load balance equation which ensures that the correct load F is applied. All equations are written in dimensionless form using the Hertzian dry contact parameters [7] (i.e. Hertzian contact pressure p_h and Hertzian contact radius a). The Reynolds [8] equation describing the dimensionless pressure distribution P for

a steady state circular contact problem with unidirectional surface velocities u_1 and u_2 in the X-direction is given by:

$$\nabla\cdot\left(\varepsilon\nabla P\right)-\frac{\partial\left(\bar{\rho}H\right)}{\partial X}=0 \tag{1}$$

Where: $\varepsilon=\dfrac{\bar{\rho}H^3}{\bar{\mu}\lambda}$, $\lambda=\dfrac{12u_m\mu_R R^2}{a^3 p_h}$, $u_m=\dfrac{u_1+u_2}{2}$ and $R=\dfrac{R_1R_2}{R_1+R_2}$

This equation stems from the Navier-Stokes equations to which the thin film simplifying assumptions are applied. H is the film thickness. The dimensionless viscosity $\bar{\mu}$ and density $\bar{\rho}$ vary with pressure throughout the contact domain Ω_c (See Figure 3) making the problem highly nonlinear. The different laws of these transport properties that are used in this work are provided in Appendix A.

Neglecting body loads, the linear elasticity equations consist in finding the displacement vector $U=\{u,v,w\}$ over the computational domain Ω such that:

$$div\left(\sigma\right)=0 \;\; with \;\; \sigma=C\;\varepsilon_s\left(U\right) \tag{2}$$

Where σ is the stress tensor, ε_s the strain tensor and C the compliance matrix. The film thickness H contains three contributions: the separation of the solid bodies H_0, the original undeformed geometry and the elastic deflection of the components δ:

$$H\left(X,Y\right)=H_0+\frac{X^2+Y^2}{2}+\delta\left(X,Y\right) \quad \text{with} \quad \delta\left(X,Y\right)=\left|w\left(X,Y\right)\right| \tag{3}$$

Finally, the load balance equation is written in dimensionless form as follows:

$$\int_{\Omega_c} P\left(X,Y\right)d\Omega=\frac{2\pi}{3} \tag{4}$$

Where $2\pi/3$ corresponds to the dimensionless external load. This equation ensures that the correct external load is applied. The latter is controlled by the value of the film thickness constant H_0.

Boundary conditions

Starting with Reynolds equation, it is admitted that p equals the ambient pressure at the boundary of the contact domain Ω_c. In practice, it is defined as zero and thus, the pressure solved for corresponds to the pressure rise above the ambient level value:

$$p=0 \quad \text{on} \;\; \partial\Omega_c \tag{5}$$

Moreover, since the lubricant is assumed to be at liquid state inside the film, pressures lower than the vapour pressure are physically impossible. The fluid will cavitate and the

pressure will remain constant and equal to the vapour pressure. Since in most situations the vapour pressure of the lubricant is of the same order of magnitude as the ambient pressure which is very small compared to the contact pressure, the Reynolds' [8] cavitation boundary condition requires that:

$$p \geq 0 \quad \text{on } \Omega_c \quad \text{and} \quad p = \nabla p \cdot \vec{n}_c = 0 \quad \text{on the cavitation boundary} \tag{6}$$

Where $\vec{n}_c$ is the outward normal vector to the outlet boundary of the contact also called cavitation boundary. It is clear that determining the exact location of this boundary (specified by the appearance of negative pressures in the solution of Reynolds' equation) is a free boundary problem since the pressure distribution is not known "a priori". It is important to note that the first part of eq. (6) ensures that the cavitation of the lubricant and the film break-up at the outlet of the contact are taken into account, whereas the second part ensures the mass conservation of the lubricant flow.

Finally, the boundary conditions of the elastic problem are defined as follows:

$$\begin{cases} U = 0 & \text{at the bottom boundary } \partial\Omega_b \\ \sigma_n = \sigma \cdot \vec{n} = -P & \text{at the contact area boundary } \Omega_c \\ \sigma_n = 0 & \text{elsewhere} \end{cases} \tag{7}$$

The boundary conditions defined in this section, associated to the different EHL equations provided in section 2.1.1 completely define the physical problem to be solved.

Geometrical and material considerations

A half-space configuration can be assumed because the size of the contact is very small compared to the size of the solids. In practice, the latter corresponds to a cube with large dimensions compared to the size of the contact. In a previous paper [5], the authors showed that the dimensions of the cube should be at least 60 times larger than the Hertzian contact radius so that it can be considered as a half-space. The contact domain Ω_c is located on the centre of the upper face of the cube and extends from *X*=-4.5 to 1.5 and *Y*=-3.0 to 3.0 (See Figure 3). Note that Reynolds equation is two-dimensional and is solved on Ω_c whereas the elasticity equations are three-dimensional and are solved on the entire cubic domain Ω.

Remark: in the line contact case, the half-space structure is a square with large dimensions compared to the contact domain which this time is one-dimensional and is also located on the centre of the upper side of the square. In addition, a plane strain analysis is applied to the linear elasticity problem.

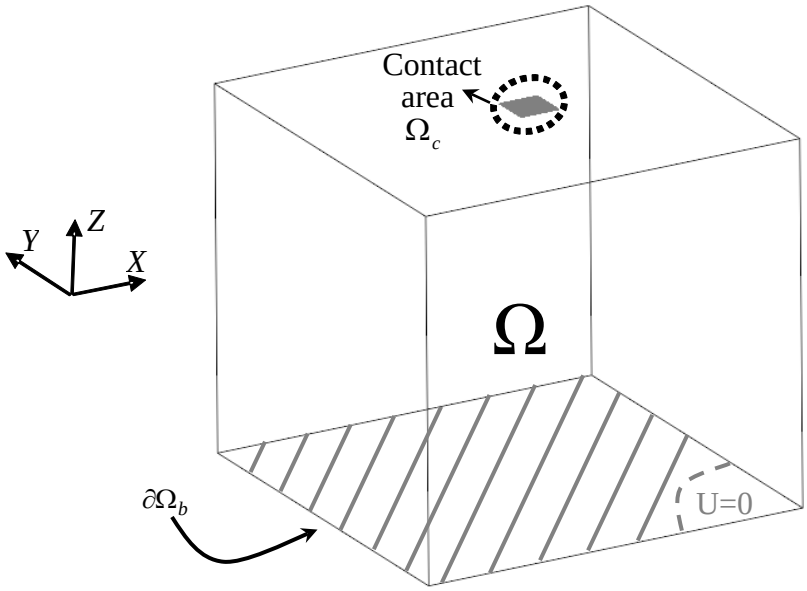

Figure 3: Geometry of the EHL problem

In order to simplify the computational model, an equivalent problem is defined to replace the elastic deformation computation for both contacting bodies under the same pressure distribution. The equivalent model is defined by applying eq. (2) to a body that has the following material properties (See Appendix B):

$$E_{eq} = \frac{E_1^2 E_2 \left(1+\upsilon_2\right)^2 + E_2^2 E_1 \left(1+\upsilon_1\right)^2}{\left[E_1\left(1+\upsilon_2\right) + E_2\left(1+\upsilon_1\right)\right]^2} \quad \text{and} \quad \upsilon_{eq} = \frac{E_1\upsilon_2\left(1+\upsilon_2\right) + E_2\upsilon_1\left(1+\upsilon_1\right)}{E_1\left(1+\upsilon_2\right) + E_2\left(1+\upsilon_1\right)}$$

Remark: For the particular case of the two contacting elements being made out of the same material (E,υ), the equivalent material properties are $E_{eq} = E/2$ and $\upsilon_{eq} = \upsilon$. Therefore, the total elastic deflection would be twice the elastic deflection of each body.

Moreover, by multiplying the equivalent Young's Modulus by a/R the dimensionless displacement vector is obtained directly and dividing it by p_h allows the use of the dimensionless pressure distribution *P* as a pressure load in the contact area. Hence, the equivalent material properties become:

$$E_{eq} = \frac{E_1^2 E_2 \left(1+\upsilon_2\right)^2 + E_2^2 E_1 \left(1+\upsilon_1\right)^2}{\left[E_1\left(1+\upsilon_2\right) + E_2\left(1+\upsilon_1\right)\right]^2} \times \frac{a}{R\,p_h} \quad \text{and} \quad \upsilon_{eq} = \frac{E_1\upsilon_2\left(1+\upsilon_2\right) + E_2\upsilon_1\left(1+\upsilon_1\right)}{E_1\left(1+\upsilon_2\right) + E_2\left(1+\upsilon_1\right)} \qquad (8)$$

The previous simplification is equivalent to considering that one of the bodies is rigid while the other (that has the equivalent material properties defined in eq. (8)) accommodates the total elastic deflection of both surfaces. This avoids running a similar calculation twice (once for every solid body).

Numerical model

This section describes the numerical model used for the modelling of EHL contacts operating under an isothermal Newtonian regime.

The penalty method

As pointed out previously, at the outlet of the contact a free boundary problem arises. It is treated by means of a **penalty method**. The latter was introduced to EHL problems by Wu [9]. This approach introduces an additional penalty term to the Reynolds equation (1) that becomes:

$$\nabla\cdot\left(\varepsilon\nabla P\right)-\frac{\partial\left(\bar{\rho}H\right)}{\partial X}-\xi\cdot P^{-}=0 \tag{9}$$

Where ξ is an arbitrary **large** positive number and $P^{-}=\min\left(P,0\right)$ corresponds to the negative part of the pressure distribution. Note that the penalty term $(-\xi\cdot P^{-})$ has no effect where $P\geq 0$ and the consistency of Reynolds' equation is preserved. However, in the outlet region of the contact, where $P<0$, the penalty term dominates eq. (9), provided that the arbitrary constant ξ has a sufficiently large value. Hence, the negative pressures are forced towards zero by the presence of the penalty term and the physical constraint that $P\geq 0$ over the entire computational domain is automatically satisfied. Wu also showed that this approach satisfies the Reynolds' boundary conditions and thus the mass flow rate conservation throughout the contact. In addition, this method is very straightforward and easy to implement.

Finite element formulations

The full-system approach used in this work consists in solving Reynolds equation, the linear elasticity equations and the load balance equation simultaneously. In the Reynolds' equation, the dimensionless film thickness *H* is replaced by its expression given in eq. (3) whereas the dimensionless viscosity $\bar{\mu}$ and density $\bar{\rho}$ are replaced by one of the expressions provided in Appendix A. The Reynolds' and linear elasticity equations are partial differential equations whereas the load balance equation is an ordinary integral equation that is added directly to the system along with the introduction of an additional unknown H_0. Hence, the unknowns of this model are the pressure distribution *P*, the elastic deformation of the contacting elements $U=\left\{u,v,w\right\}$ and the film thickness constant H_0.

- **Galerkin formulation**

A standard Galerkin formulation is applied to the Reynolds' and linear elasticity equations. The latter is obtained by multiplying each equation by a given weighting function, W_P and W_U respectively, and integrating it over the corresponding domain of application. Finally, integration by parts is applied to the equations revealing thus the boundary terms. For the sake of simplicity, the zero boundary terms are omitted. The load balance equation is weighted by W_{H_0}. The resultant system of equations becomes:

Find $(P,U,H_0) \in S_P \times S_U \times R$ such that $\forall (W_P, W_U, W_{H_0}) \in S_P \times S_U \times R,$ one has:

$$\begin{cases} \int_{\Omega_c} -\varepsilon \nabla P \cdot \nabla W_P \, d\Omega + \int_{\Omega_c} \bar{\rho} H \frac{\partial W_P}{\partial X} d\Omega - \int_{\Omega_c} \xi \cdot P^{-} W_P \, d\Omega = 0 \\ \int_{\Omega} -C \varepsilon_s (U) \cdot \varepsilon_s (W_U) d\Omega + \int_{\Omega_c} -P \cdot \vec{n} \, W_U \, d\Omega = 0 \\ \int_{\Omega_c} P W_{H_0} d\Omega - \frac{2\pi}{3} W_{H_0} = 0 \end{cases} \tag{10}$$

Where: $S_P = \{ P \in H^1(\Omega_c) / P = 0 \text{ on } \partial\Omega_c \}$ and $S_U = \{ U \in H^1(\Omega) / U = 0 \text{ on } \partial\Omega_b \}$

Note that Reynolds' equation is solved on the two-dimensional contact domain Ω_c whereas the linear elasticity equations are solved on the three-dimensional domain Ω.

- **Approximated formulation**

Let us now write the discrete form of the previous system of equations. Consider $\Omega^h = \{\Omega_1, ..., \Omega_{n_e}\}$ a finite element partition of Ω such that: $\bar{\Omega} = \cup_{e=1}^{n_e} \bar{\Omega}_e$, $\bar{\Omega} = \Omega \cup \partial\Omega$, $\bar{\Omega}_e = \Omega_e \cup \partial\Omega_e$ and $\Omega_e \cap \Omega_{e'} = \phi$ if $e \neq e'$. n_e denotes the total number of elements in the partition while $\partial\Omega$ and $\partial\Omega_e$ denote respectively the boundaries of the domain Ω and the element Ω_e. Let Ω_{ce} be the set of elements defined by $\Omega_{ce} = \{\Omega_e \cap \Omega_c / \Omega_{ce} \neq \varnothing\}$ and let n_{ce} be the total number of elements belonging to Ω_{ce}. Let $S_P^h \subset S_P$ and $S_U^h \subset S_U$. The discrete functions P^h and U^h defining these spaces have the same characteristics as their analytical equivalents P and U defined in the previous section. Moreover, $P^h \in L^l$ and $U^h \in L^{l'}$ where L^l and $L^{l'}$ are the sets of piecewise polynomials of degrees equal to l and l' respectively defined within each element Ω_e. The approximate functions $P^{h(e)}$ and $U^{h(e)}$ (within an element *e*) of *P* and *U* respectively, are given by:

$$P^{h(e)} = \sum_{i=1}^{n_P} P_i^{(e)} N_{Pi} \quad \text{and} \quad U^{h(e)} = \sum_{i=1}^{n_U} U_i^{(e)} N_{Ui} \tag{11}$$

Where $P_i^{(e)}$ and $U_i^{(e)}$ are the nodal values of *P* and *U* respectively, associated to the interpolation functions N_{Pi} and N_{Ui} within the element *e* (n_P and n_U being their respective numbers). The weighting functions W_P and W_U are approximated in a similar way by $W_P^{h(e)}$ and $W_U^{h(e)}$ respectively:

$$W_P^{h(e)} = \sum_{i=1}^{n_P} W_{Pi}^{(e)} N_{Pi} \quad \text{and} \quad W_U^{h(e)} = \sum_{i=1}^{n_U} W_{Ui}^{(e)} N_{Ui} \tag{12}$$

Where $W_{P,i}^{(e)}$ and $W_{U,i}^{(e)}$ are the nodal values of the weight functions W_P and W_U within the element *e* respectively. The discrete form of the system of equations (10) is obtained by replacing the field variables *P* and *U* by their discrete equivalents P^h and U^h respectively and the weighting functions W_P and W_U by W_P^h and W_U^h respectively:

$$\text{Find } \left(P^h, U^h, H_0\right) \in S_P^h \times S_U^h \times R \text{ such that } \forall \left(W_P^h, W_U^h, W_{H_0}\right) \in S_P^h \times S_U^h \times R, \text{ one has:}$$

$$\begin{cases} \int\limits_{\Omega_c^h} -\varepsilon \nabla P^h \cdot \nabla W_P^h d\Omega + \int\limits_{\Omega_c^h} \overline{\rho} H \dfrac{\partial W_P^h}{\partial X} d\Omega - \int\limits_{\Omega_c^h} \xi \cdot P^h W_P^h d\Omega = 0 \\ \int\limits_{\Omega^h} -C\varepsilon_s\left(U^h\right) \cdot \varepsilon_s\left(W_U^h\right) d\Omega + \int\limits_{\Omega_c^h} -P^h \cdot \vec{n}\, W_U^h d\Omega = 0 \\ \int\limits_{\Omega_c^h} P^h W_{H_0} d\Omega - \dfrac{2\pi}{3} W_{H_0} = 0 \end{cases} \tag{13}$$

Again, for the sake of simplicity, the zero boundary integrals have been omitted. The unknowns of the discrete system of equations (13) are the nodal values of *P* and *U* and the value of the film thickness constant parameter H_0.

Remark: The circular contact problem is symmetric with respect to the *ZX*-plane. This symmetry is taken into account in order to reduce its size. Hence, the linear elasticity problem requires a symmetry boundary condition on the symmetry plane *ZX* ($U \cdot \vec{n} = 0 \Leftrightarrow v = 0$ on $\partial\Omega_s$). Similarly, Reynolds' equation requires an additional symmetry boundary condition ($\nabla P \cdot \vec{n} = 0 \Leftrightarrow \partial P / \partial Y = 0$ on $\partial\Omega_{cs}$) and the computed dimensionless load should equal $\pi/3$ instead of $2\pi/3$.

Stability issues

The solution of Reynolds equation is known to be unstable in the central contact area (high pressure region) for highly loaded contacts [10-14]. In this section, we provide a method to cure these instabilities that lead to an oscillatory behaviour of the solution. The line contact case is also treated for demonstrative purposes. In fact, let us rewrite the Reynolds equation in a different way:

$$R(P) = -\nabla \cdot \left(\varepsilon \nabla P\right) + H \frac{\partial \overline{\rho}}{\partial P} \frac{\partial P}{\partial X} + \overline{\rho} \frac{\partial H}{\partial X} = 0 \tag{14}$$

Let $\beta = \beta_X$ in the line contact case or $\beta = \{\beta_X, \beta_Y\}$ in the circular contact case with $\beta_X = H \dfrac{\partial \overline{\rho}}{\partial P}$ and $\beta_Y = 0$. Finally, let $Q = -\overline{\rho} \dfrac{\partial H}{\partial X}$, then eq. (14) can be written:

$$R(P) = \underbrace{-\nabla \cdot \left(\varepsilon \nabla P\right)}_{\text{«Diffusion »}} + \underbrace{\beta \cdot \nabla P}_{\text{«Convection »}} \underbrace{- Q}_{\text{« Source »}} = 0 \tag{15}$$

The penalty term is not mentioned for the sake of simplicity and because it is nil in the region of interest of this section (high pressure region). But keep in mind that this term should be added to eq. (15) during the resolution process. Note that eq. (15) is the Reynolds' equation in compact notation for both line and circular contacts. For the line contact case, the differential operators are unidirectional in the *X*-direction whereas in the circular contact case they are bidirectional (in the *X* and *Y*-directions).

Equation (15) has the form of the classical Diffusion-Convection equation (applied to *P*) with a source term *Q*. We can clearly identify the diffusion term (left) with a diffusion coefficient ε and the convection term (centre) with a convection operator $\beta \cdot \nabla$. For highly loaded contacts, ε becomes very small. In fact, $\overline{\rho}$ exhibits a slight increase while $\overline{\mu}$ is increased by several orders of magnitude and *H* becomes smaller. Therefore, the convection-like term in eq. (15) becomes dominant. It is well known that the standard Galerkin formulation, associated with the finite element method works well only when the diffusion term is dominant [15-18]. In fact, the central differencing property of the Galerkin method is well suited only for elliptic problems (dominated by diffusion). When convection becomes dominant, the Galerkin formulation is no longer appropriate and gives rise to spurious oscillations in the solution. One way to get rid of these oscillations is obtained by using special stabilized formulations. A various number of these techniques can be found in the literature such as "artificial diffusion" [15, 17, 19] or "Discontinuous Galerkin" methods [20, 21]. In the following, we propose the use of "artificial diffusion" techniques to cure the spurious oscillations of the solution for highly loaded contacts.

- **Line contact**

As mentioned earlier, in the case of a highly loaded contact, Reynolds equation becomes convection-dominated. The solution exhibits an oscillatory behaviour (See Figure 4, Left). In order to overcome such a problem Brooks and Hughes [15] introduced the so called Streamline Upwind Petrov Galerkin (SUPG) method. The discrete weak variational form for the SUPG method applied to Reynolds equation (15) is given by:

$$\begin{aligned} &\text{Find } P^h \in S_P^h \text{ such that } \forall W_P^h \in S_P^h, \text{ one has:} \\ &\int_{\Omega_c^h} \varepsilon \nabla P^h \cdot \nabla W_P^h d\Omega + \int_{\Omega_c^h} \left(\beta \cdot \nabla P^h - Q\right) W_P^h d\Omega \\ &\qquad + \sum_{e=1}^{n_{ce}} \int_{\Omega_{ce}} R\left(P^h\right) \tau \left(\beta \cdot \nabla W_P^h\right) d\Omega = 0 \end{aligned} \tag{16}$$

The first two terms represent the standard Galerkin method applied to Reynolds equation while the last term represents the additional stabilizing term that is added to the interior Ω_{ce} of each discretization element.

Another interesting technique was proposed by Hughes et al. [17] based on the fact that stabilization terms may be obtained by minimizing the square of the equation's residual. It is called the Galerkin Least Squares (GLS) method. The discrete weak variational form for this method is given by:

Find $P^h \in S_P^h$ such that $\forall W_P^h \in S_P^h$, one has:

$$\int_{\Omega_c^h} \varepsilon \nabla P^h \cdot \nabla W_P^h d\Omega + \int_{\Omega_c^h} \left(\beta \cdot \nabla P^h - Q\right) W_P^h d\Omega + \sum_{e=1}^{n_{ce}} \int_{\Omega_{ce}} R\left(P^h\right) \tau \left(\beta \cdot \nabla W_P^h - \nabla \cdot \left(\varepsilon \nabla W_P^h\right)\right) d\Omega = 0 \tag{17}$$

Once again, we can identify the standard Galerkin formulation in the first two terms and the additional stabilizing term in the last part. The most important feature of SUPG and GLS is that both are residual based techniques. In other words, they do not affect the solution of the original problem. Actually, the additional terms vanish at the converged solution ($R \approx 0$) and therefore the consistency of Reynolds equation is preserved.

The definition of the tuning parameter τ remained "intuitive" for a long time. An example of a theoretical formulation was introduced by Hughes [18] in the mid 90's. Since, several formulations have been proposed by various authors. In this work we shall adopt the definition given by Galeão et al. [16] who provided an extension of this parameter to high order approximations:

$$\tau = \frac{h_e}{2|\beta| l} \xi\left(P_e\right)$$
$$\text{with: } P_e = \frac{|\beta| h_e}{2 \varepsilon l} \text{ and } \xi\left(P_e\right) = \coth\left(P_e\right) - \frac{1}{P_e} \tag{18}$$

Where h_e and P_e are respectively the characteristic length and the local Peclet number of the element *e*. P_e defines the convection-to-diffusion ratio inside an element *e*. Whenever $P_e > 1$, convection becomes dominant and stability problems mentioned earlier are likely to occur.

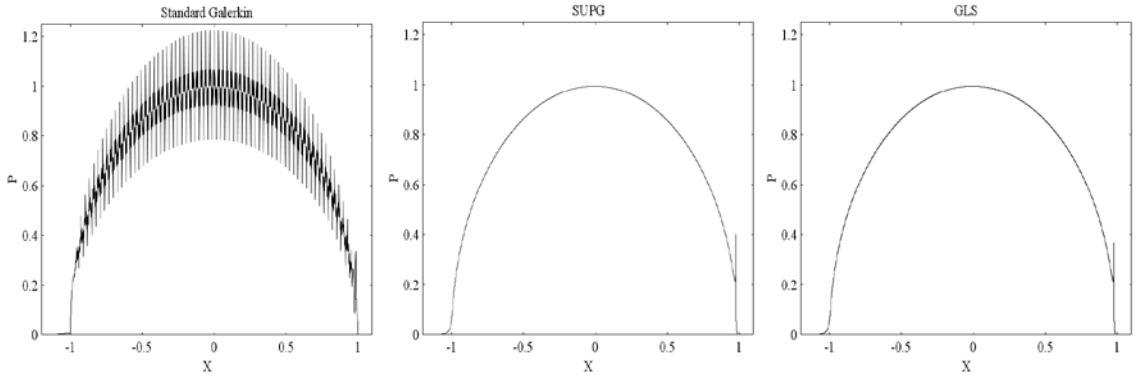

Figure 4: Heavily loaded line contact problem and the effect of stabilization. Left: Standard Galerkin, Centre: SUPG, Right: GLS (p_h=3 GPa, μ_R=0.012 Pa.s, α^*=23 GPa^{-1}, u_1=u_2= 1m/s, R=15 mm, A_1=19.17 °C, A_2=4.07x10^{-3} MPa^{-1}, B_1=0.23, B_2=0.0249 MPa^{-1}, C_1=16.04, C_2=18.18 °C, $T_g(0)$=-73.86 °C, μ_g=10^{12} Pa.s and T=40 °C)

Figure 4 shows a typical case of a heavily loaded steel-steel line contact. Lagrange quintic elements are used for the hydrodynamic problem and quadratic elements for the elastic part, with a mesh density of 400 elements in the Hertzian contact region ($-1 \le X \le 1$). The total

number of dofs is 23000 where only 2000 dofs are dedicated to the hydrodynamic part and the rest to the elastic calculation. This is to be expected since the former is one dimensional while the latter is two dimensional. The Dowson & Higginson [22] formula and the WLF [23] model (See Appendix A) are used as density-pressure and viscosity-pressure relationships respectively. The solution exhibits an oscillatory behaviour when a Standard Galerkin formulation is used. On the other hand, the use of SUPG or GLS formulations completely smoothes out this spurious behaviour.

Remark: Using high order elements for the hydrodynamic problem, as an alternative to refining the mesh, allows having a good precision for its solution without inducing any unnecessary increase in the number of dofs of the two-dimensional (line contact case) or three-dimensional (circular contact case) elastic problem.

- **Circular contact**

In the case of a heavily loaded circular contact problem, the same behaviour is observed for a standard Galerkin formulation and the solution exhibits serious oscillations in the central area of the contact as can be seen in Figure 5 (Left). The SUPG and GLS formulations are the same as those given in eqs. (16) and (17) respectively. But in this case, both methods only succeed in reducing the amplitude of the oscillations without completely smoothing them out as can be seen in Figure 5 (Centre). In the two dimensional case of the convection-diffusion equation, it is of common use to add additional terms to the stabilized SUPG or GLS formulations such as "Isotropic Diffusion (ID)" terms [24]. The latter succeed in smoothing out the remaining oscillations without a significant perturbation in the solution of the original problem. These terms are defined as:

$$ID = \sum_{e=1}^{n_{ce}} \int_{\Omega_{ce}} \rho_{id} \frac{h_e |\beta|}{2l} \nabla P^h \cdot \nabla W_P^h \, d\Omega \tag{19}$$

The coefficient ρ_{id} represents the relative amount of "Isotropic Diffusion" with respect to the original method. The terms in eq. (19) are added to the stabilized SUPG or GLS formulations given in eqs. (16) and (17) respectively.

Figure 5 shows the case of a heavily loaded steel-steel point contact. The same lubricant is used as in the line contact case with the same viscosity-pressure and density-pressure relationships (See previous section). This case corresponds to a severe EHL contact that can rarely be found in real life contacts. Therefore, it has no important physical relevance, but it is used here in the only purpose of demonstrating the stability of the current model. Lagrange quintic elements are used for the hydrodynamic problem and quadratic elements for the elastic part. The total number of dofs is 75000 where 35000 dofs are dedicated to the hydrodynamic part and the rest to the elastic calculation. The solution exhibits an oscillatory behaviour when a Standard Galerkin formulation is used. The use of SUPG or GLS formulations reduces these oscillations without completely smoothing them out. And finally, the addition of "Isotropic Diffusion" terms eliminates the remaining oscillations in the solution (ρ_{id} is set to 0.5).

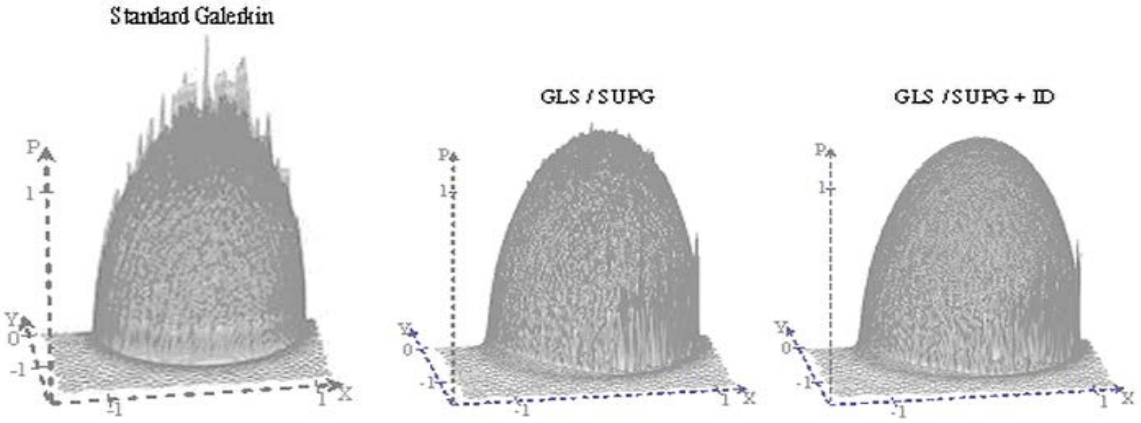

Figure 5: Heavily loaded circular contact problem and the effect of stabilization. Left: Standard Galerkin, Centre: SUPG/GLS, Right: SUPG/GLS+ID (p_h=3 GPa, μ_R=0.012 Pa.s, α^*=23 GPa^{-1}, u_1=u_2= 1m/s, R=12.7 mm, A_1=19.17 °C, A_2=4.07x10^{-3} MPa^{-1}, B_1=0.23, B_2=0.0249 MPa^{-1}, C_1=16.04, C_2=18.18 °C, $T_g(0)$=-73.86 °C, μ_g=10^{12} Pa.s and T=40 °C)

It is important to note that the ID terms are non-residual based and therefore the consistency of the Reynolds equation is lost. But, fortunately, the addition of these terms to the stabilized formulations does not significantly affect the solution of the original problem as can be seen in Figure 6. In order to evaluate the effect of these terms on the solution of the circular contact problem, a test case was carried out under the same conditions mentioned earlier with the only difference that the Hertzian pressure is taken to be 0.68 GPa. This allows getting the standard Galerkin solution (the contact is not heavily loaded) in order to compare it to the stabilized GLS formulation with / without addition of "Isotropic Diffusion".

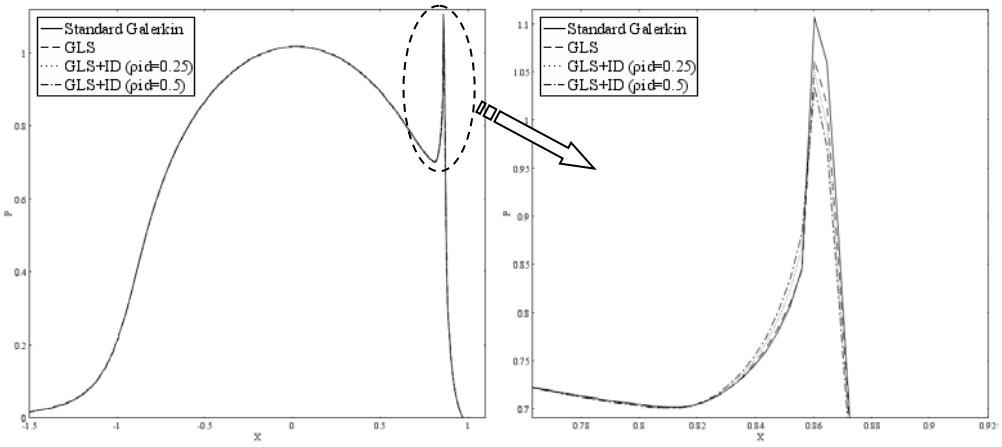

Figure 6: Effect of « Isotropic Diffusion » on the dimensionless pressure solution of Reynolds' equation in the case of a circular contact (p_h=0.68 GPa, μ_R=0.012 Pa.s, α^*=23 GPa^{-1}, u_1=u_2=1m/s, R=12.7 mm, A_1=19.17 °C, A_2=4.07x10^{-3} MPa^{-1}, B_1=0.23, B_2=0.0249 MPa^{-1}, C_1=16.04, C_2=18.18 °C, $T_g(0)$=-73.86 °C, μ_g=10^{12} Pa.s and T=40 °C)

Figure 6 shows the dimensionless pressure profile along the central line in the X-direction for the case mentioned earlier. Globally, the additional ID terms do not significantly affect the solution (Left). By zooming on the pressure spike's region (Right) we can note that a slight difference can be observed in this region. Finally, note that the more "Isotropic Diffusion" is added, the more the pressure spike is affected. In fact, for $\rho_{id} = 0.5$, the pressure spike deviates from that of the standard Galerkin or GLS solutions more than for $\rho_{id} = 0.25$. The dimensionless central and minimum film thicknesses H_c and H_m along with their

corresponding relative deviations for the different formulations with respect to the standard Galerkin solution are reported in Table 1:

	H_c	H_m	$(\Delta H/H)_c$	$(\Delta H/H)_m$
Standard Galerkin	0.137462	0.074807	-	-
GLS	0.136897	0.074519	0.41 %	0.38 %
GLS+ID (ρ_{id}=0.25)	0.136752	0.074469	0.52 %	0.45 %
GLS+ID (ρ_{id}=0.5)	0.136608	0.074419	0.62 %	0.52 %

Table 1: Effect of « Isotropic Diffusion » on the dimensionless film thickness results in the case of a circular contact (p_h=0.68 GPa, μ_R=0.012 Pa.s, α^*=23 GPa^{-1}, u_1=u_2=1m/s, R=12.7 mm, A_1=19.17 °C, A_2=4.07x10^{-3} MPa^{-1}, B_1=0.23, B_2=0.0249 MPa^{-1}, C_1=16.04, C_2=18.18 °C, $T_g(0)$=-73.86 °C, μ_g=10^{12} Pa.s and T=40 °C)

Table 1 clearly confirms that the effect of the additional ID terms on the film thickness results is also negligible and that, again, the more ID is added, the more the solution is affected. From here on, unless stated otherwise, whenever "Isotropic Diffusion" is employed, a value of $\rho_{id} = 0.5$ is considered.

Remark: Note that, a single formulation can be used for both lightly and heavily loaded contacts, since the stabilized formulations introduced earlier do not affect the solution of the former.

2.2.3 Newton-Raphson procedure

A Newton (Newton-Raphson) procedure is applied to the non-linear system of equations formed by the stabilized Reynolds equation, the linear elasticity equations and the load balance equation. This system can be rewritten under the following matrix form:

$$\begin{cases} R_{stab}\left(P,U,H_0\right) = 0 \\ J_{21}P + J_{22}U = 0 \\ J_{31}P = F_3 \end{cases} \tag{20}$$

Where $\left(P,U,H_0\right)$ is the vector of the nodal values of P and U, and the constant film thickness parameter H_0. $R_{stab}\left(P,U,H_0\right)$ denotes the discrete form of the non-linear stabilized Reynolds equation. It is approximated by its linear part $L_{P,U,H_0}R_{stab}\left(\delta P,\delta U,\delta H_0\right)$ at $\left(P,U,H_0\right)$ obtained by a first order Taylor expansion:

$$\begin{aligned} L_{P,U,H_0}R_{stab}\left(\delta P,\delta U,\delta H_0\right) = R_{stab}\left(P,U,H_0\right) &+ \left.\frac{\partial R_{stab}}{\partial P}\right|_{P,U,H_0}\delta P \\ &+ \left.\frac{\partial R_{stab}}{\partial U}\right|_{P,U,H_0}\delta U + \left.\frac{\partial R_{stab}}{\partial H_0}\right|_{P,U,H_0}\delta H_0 \end{aligned} \tag{21}$$

Let: $J_{11} = \left.\frac{\partial R_{stab}}{\partial P}\right|_{P,U,H_0}$, $J_{12} = \left.\frac{\partial R_{stab}}{\partial U}\right|_{P,U,H_0}$ and $J_{13} = \left.\frac{\partial R_{stab}}{\partial H_0}\right|_{P,U,H_0}$

The elasticity and load balance equations are already linear and therefore they are strictly equivalent to their linear part at (P,U,H_0). Starting with an initial guess (P^0,U^0,H_0^0) of the solution, the linearized system of equations to solve at the i^{th} iteration of the Newton procedure is defined by:

$$\text{Find } \left(\delta P^i,\delta U^i,\delta H_0^i\right) \text{ such that: } \begin{cases} L_{P^{i-1},U^{i-1},H_0^{i-1}} R_{stab}\left(\delta P^i,\delta U^i,\delta H_0^i\right)=0 \\ J_{21}\cdot\left(P^{i-1}+\delta P^i\right)+J_{22}\cdot\left(U^{i-1}+\delta U^i\right)=0 \\ J_{31}\cdot\left(P^{i-1}+\delta P^i\right)=F_3 \end{cases} \tag{22}$$

Where $\left(\delta P^i,\delta U^i,\delta H_0^i\right)$ is an increment vector. The Hertzian pressure and elastic deformation profiles or a previously stored solution are a good estimate for (P^0,U^0). Replacing $L_{P^{i-1},U^{i-1},H_0^{i-1}} R_{stab}\left(\delta P^i,\delta U^i,\delta H_0^i\right)$ by its expression provided in eq. (21), the system of equations (22) becomes:

$$\begin{bmatrix} J_{11} & J_{12} & J_{13} \\ J_{21} & J_{22} & \varnothing \\ J_{31} & \varnothing & \varnothing \end{bmatrix}^{i-1} \begin{Bmatrix} \delta P \\ \delta U \\ \delta H_0 \end{Bmatrix}^{i} = \begin{Bmatrix} -R_{stab}\left(P,U,H_0\right) \\ -J_{21}P-J_{22}U \\ F_3-J_{31}P \end{Bmatrix}^{i-1} \tag{23}$$

The matrix on the left hand side is the Jacobian matrix where we can identify the coupling terms J_{12}, J_{13}, J_{21} and J_{31}. We remind the reader that in the present approach the Jacobian matrix is sparse (more than 99 % of the terms are zeros), and therefore the computational effort or memory usage required for inverting it are far less important than for a full matrix. The Newton procedure consists in solving the linearized system of eqs. (23) at every iteration i and adding the result $\left(\delta P^i,\delta U^i,\delta H_0^i\right)$ to the vector $\left(P^{i-1},U^{i-1},H_0^{i-1}\right)$ obtained at the previous iteration:

$$\begin{Bmatrix} P \\ U \\ H_0 \end{Bmatrix}^{i} = \begin{Bmatrix} P \\ U \\ H_0 \end{Bmatrix}^{i-1} + \begin{Bmatrix} \delta P \\ \delta U \\ \delta H_0 \end{Bmatrix}^{i} \tag{24}$$

This system is solved using a direct solver and the procedure is repeated until the convergence of the solution is reached i.e. until the Euclidian norm of the relative residual error vector falls below 10^{-6}.

2.3 Quantitative analysis

In this section, a thorough quantitative analysis of the current model is described. First, the effect of the penalty term on the pressure and film thickness solutions is analyzed then, a comparative study with a finite difference based model (using multigrid techniques) is carried out for a typical circular contact case. The latter validates the current approach and proves its efficiency.

2.3.1 Penalty term analysis

In section 2.2.1, it was pointed out that the free boundary problem that arises at the outlet of the contact is treated by applying a penalty method. In this section, the effect of the penalty term on the pressure and film thickness solutions is analyzed. For this purpose a typical steel-steel ball on plane contact is considered. The lubricant is assumed to be compressible. Its density varies with pressure according to the Dowson & Higginson formula (See Appendix A). The Roelands [25] model is used for viscosity-pressure dependence. The parameter ρ_{id} is taken to be 0.5. Lagrange quintic elements are used for the hydrodynamic problem and quadratic elements for the elastic part. The mesh size is approximately equal to 0.5 in the inlet and outlet regions of the contact and 0.05 in the central area. In practice, the penalty term's parameter ξ in eq. (9) is taken as:

$$\xi = \xi_0 \times h_e^2 \tag{25}$$

Where ξ_0 is an arbitrary large positive number. The values of the central and minimum film thicknesses, the outlet absicca of the contact (location of the free boundary X_{out}) on the central line in the *X*-direction and the minimum pressure are listed in Table 2 as a function of the value of ξ_0.

ξ_0	H_c	H_m	X_{out} (Y=0)	Min(P)
10^2	0.082198	0.038382	0.9870	$-3.0092.\ 10^{-2}$
10^4	0.082214	0.039267	1.0403	$-2.5630.\ 10^{-3}$
10^6	0.082215	0.039298	1.0589	$-9.5199.\ 10^{-5}$
10^8	0.082215	0.039298	1.0602	$-6.5941.\ 10^{-5}$

Table 2: Effect of the penalty term on the pressure and film thickness solutions (F=100N, p_h=1 GPa, u_1=u_2=0.8 m/s, R=16 mm, μ_R=0.04 Pa.s, α=22 GPa^{-1} and T=T_0=T_R=20 °C)

It is clear that a minimum value of ξ_0 is required in order to get converged pressure and film thickness solutions. In fact, note that beyond $\xi_0 = 10^6$, any increase of the value of this parameter is useless and does not lead to any significant changes in the solution. This is why this value has been employed throughout this work. The condition number of the linear system is of course influenced by the latter. As a direct linear system solver is used, it does not affect the solution. Finally, note that the larger this parameter is, the closer the negative pressures get to zero.

2.3.2 Validation and comparison with FD multigrid based model

A comparative study between the present finite element model and a semi-system finite difference (with multigrid techniques) model is established. For this purpose, a representative test case corresponding to a fairly loaded circular contact problem is taken from [26] in order to compare the results and efficiency of both models. The lubricant properties and operating conditions are the same as described in the previous section. The test is carried out for several mesh sizes and the results are reported in Table 3. In fact, for the finite difference based model, the mesh diameter h_e is constant throughout the contact domain and equal to 0.046875, 0.0234375 and 0.01171875 for the three cases mentioned in Table 3 respectively whereas for the current model, h_e is variable (See Figure 7), and approximately equal to 0.5 in the inlet and outlet regions of the contact in the three test cases whereas in the central part of the contact it is approximately equal to 0.15, 0.075 and 0.05 respectively.

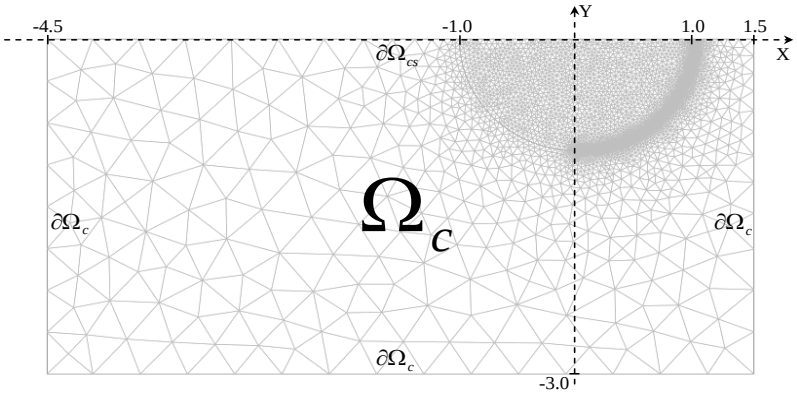

Figure 7: Meshing of the contact area Ω_c

Figure 7 shows a typical meshing of the contact area Ω_c, delimited by its boundaries $\partial\Omega_c$ and $\partial\Omega_{cs}$, for a circular contact problem. Note that the mesh is coarse in the inlet and outlet regions of the contact where the solution shows very small variations. On the other hand, a fine mesh is used in the central (Hertzian) contact area where the pressure gradients are more important. Finally, a finer mesh is used at the outlet of the central contact area where the pressure spike and film thickness constriction are generally observed. Thus a good capture of the severe pressure gradients that occur in this area is obtained.

Venner & Lubrecht [26]				Current model			
N° dofs	H_c	H_m	N_{iter}	N° dofs	H_c	H_m	N_{iter}
16 770 (128x128 mesh)	0.07887	0.03712	153	18 313	0.080950	0.038818	11
66 306 (256x256 mesh)	0.08093	0.03848	107	39 836	0.081845	0.039165	13
263 682 (512x512 mesh)	0.08144	0.03876	80	76 249	0.082215	0.039298	14

Table 3: Comparison of the current model with the Venner & Lubrecht [26] model for a typical circular contact case (F=100N, p_h=1 GPa, u_1=u_2=0.8 m/s, R=16 mm, μ_R=0.04 Pa.s, α=22 GPa^{-1} and T=T_0=T_R=20 °C)

Table 3 gives the dimensionless central and minimum film thicknesses obtained by both the Venner & Lubrecht and the current models for the test case described earlier using different mesh densities. The number of iterations N_{iter} required by each model to reach the converged solution is also reported. For the multigrid based model, N_{iter} corresponds to the equivalent number of iterations that would be carried out over the finest mesh level given in the left column. The total number of dofs for the Venner & Lubrecht model is divided by 2 with respect to the number given in [26] because this model does not take into account the symmetry of the problem (e.g.: 66306=(256+1)x(**256/2**+1)x2). Note that even for a total number of 18313 dofs, the solution given by the current model can be considered sufficiently accurate compared to the finest mesh case considered here. Also note, compared to the Venner & Lubrecht model, the much smaller number of iterations that is required to get a converged solution. This reveals the outstanding convergence rate mentioned earlier.

The 3D dimensionless pressure profile for this case is given in Figure 8 (Left) and the corresponding plot of the dimensionless pressure and film thickness profiles along the central line in the *X*-direction are shown in Figure 8 (Right).

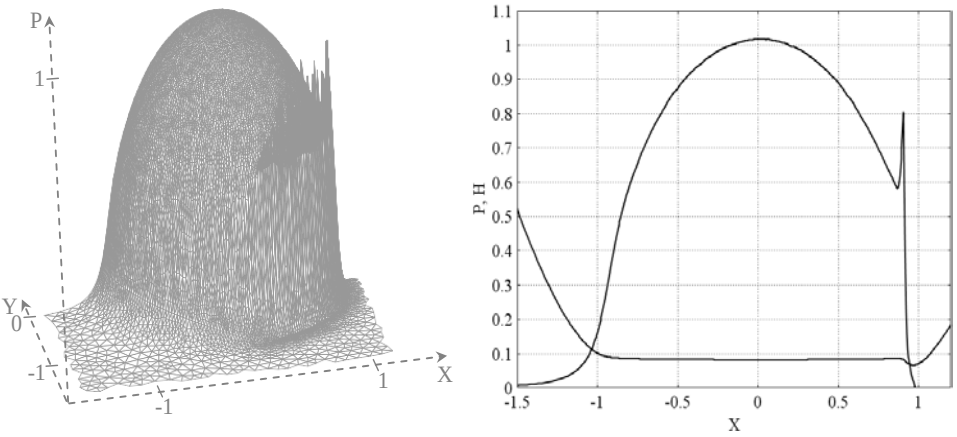

Figure 8: 3D dimensionless pressure profile (Left), dimensionless pressure and film thickness profiles along the central line in the *X*-direction (Right) (F=100N, p_h=1 GPa, u_1=u_2=0.8 m/s, R=16 mm, μ_R=0.04 Pa.s, α=22 GPa^{-1} and T=T_0=T_R=20 °C)

This test allows the validation of the current model and shows that the size of the system of equations to solve can be reduced compared to finite difference based models. This is mainly due to the use of the finite element method which enables non-regular non-structured meshing. Therefore, fine meshing is used only where needed as can be seen in Figure 7. Moreover, in a previous work [5], the authors showed that both models have the same complexity and since much faster convergence rates are obtained, then memory storage and computational time are considerably reduced. In fact, a typical circular contact resolution takes, roughly speaking, between 1 and 3 minutes on a PC with a 2 GHz processor whereas a line contact solution is obtained in less than 10 seconds.

3 Extension to a more physical modelling

In this section, the previously described model is extended to a more physical modelling of the contact's behaviour. First, non-Newtonian lubricants are considered and then thermal effects are taken into account. Both extensions introduce additional physics to the problem, making it more complex, both on the numerical and the physical level.

3.1 Non-Newtonian effects

The classical isothermal EHL theory presented in section 2 assumes that the lubricant behaves as a Newtonian fluid. However, when a non-Newtonian lubricant is used, its viscosity varies in the thickness of the film due to shear stress variations. In general, non-Newtonian lubricants have a shear-thinning behaviour. In other words, their viscosity decreases with the increase of shear stress. In the current work, this behaviour is modelled using the modified version of the Carreau equation provided by Bair [27] (See Appendix A). The latter is a very powerful shear-thinning model that takes into account the second Newtonian plateau that can occur at very high shear rates (See figure 9).

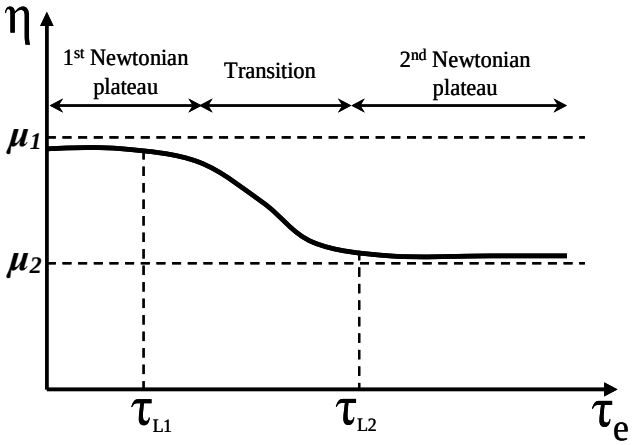

Figure 9: Typical behaviour of a non-Newtonian lubricant modelled by the Carreau model

In order to account for the viscosity variations in the film thickness, Najji [28] introduced a generalized Reynolds equation that can be written in the following dimensionless form:

$$\nabla\cdot\left(\varepsilon'\nabla P\right)-\frac{\partial\left[\bar{\rho}H\left(u_2-\frac{\bar{\eta}_e}{\bar{\eta}_e'}\left(u_2-u_1\right)\right)\right]}{\partial X}=0 \tag{26}$$

Where: $\varepsilon'=\frac{\bar{\rho}H^3}{\lambda'}\left(\frac{1}{\bar{\eta}_e''}-\frac{\bar{\eta}_e}{\bar{\eta}_e'^2}\right)$, $\lambda'=\frac{R^2\mu_R}{p_h a^3}$, $\frac{1}{\bar{\eta}_e}=\int_0^1\frac{dZ}{\bar{\eta}}$, $\frac{1}{\bar{\eta}_e'}=\int_0^1\frac{Z}{\bar{\eta}}dZ$ and $\frac{1}{\bar{\eta}_e''}=\int_0^1\frac{Z^2}{\bar{\eta}}dZ$

Note that if the generalized Newtonian viscosity η is replaced by the Newtonian one μ eq. (26) becomes the classical Reynolds equation. Finally, eq. (26) can be written in the following form:

$$\begin{aligned}R'\left(P\right)=-\nabla\cdot\left(\varepsilon'\nabla P\right)+H\left(u_2-\frac{\bar{\eta}_e}{\bar{\eta}_e'}\left(u_2-u_1\right)\right)\frac{\partial\bar{\rho}}{\partial P}\frac{\partial P}{\partial X}\\ +\bar{\rho}\frac{\partial\left[H\left(u_2-\frac{\bar{\eta}_e}{\bar{\eta}_e'}\left(u_2-u_1\right)\right)\right]}{\partial X}=0\end{aligned} \tag{27}$$

Let: $\beta_X'=H\left(u_2-\frac{\bar{\eta}_e}{\bar{\eta}_e'}\left(u_2-u_1\right)\right)\frac{\partial\bar{\rho}}{\partial P}$, $\beta_Y'=0$ and $Q'=-\bar{\rho}\frac{\partial\left[H\left(u_2-\frac{\bar{\eta}_e}{\bar{\eta}_e'}\left(u_2-u_1\right)\right)\right]}{\partial X}$

Then eq. (27) becomes:

$$R'\left(P\right)=-\nabla\cdot\left(\varepsilon'\nabla P\right)+\beta'\cdot\nabla P-Q'=0 \tag{28}$$

Hence, the generalized Reynolds' equation also has the form of a classical Diffusion-Convection equation (applied to P) with a source term Q'. Again, thermal effects are

neglected and temperature is considered constant throughout the lubricant film and equal to the ambient temperature T_0.

3.1.1 Finite element procedure

The system of EHL equations formed by the generalized Reynolds' equation, the linear elasticity and the load balance equation is solved using a similar Newton Raphson approach as described earlier. The finite element formulations for this system are not reminded here. Those are similar to the ones provided in section 2 since the generalized Reynolds equation also has the form of a convection / diffusion equation. The free boundary problem is again treated by applying a penalty method and for heavy loads, the problem exhibits similar instability features as described in section 2.2.3. This can be seen in Figure 10 where a test case is carried out with a typical shear thinning lubricant for a steel-on-glass circular contact. Note that, in practice, this case can never be realized on an experimental apparatus because glass would not withstand such a load. The Tait-Doolittle [29-30] free volume model (See Appendix A) is used to express the density and viscosity dependence on pressure. The lubricant properties can be found in Table 4.

Lubricant properties	
$\mu_{1,R}$=0.0705 Pa.s	a_v=7.52x10^{-4} °C^{-1}
$\mu_{2,R}$=0.0157 Pa.s	K'_{0R}=11.29
G_c=0.01 MPa	β'_K=0 K^{-1}
n_c=0.8	K_{0R}=8.375 GPa
B=4.2	β_K=0.006765 K^{-1}
R_0=0.658	ε_c=-9.599x10^{-4} °C^{-1}

Table 4: Lubricant properties for the non-Newtonian test case

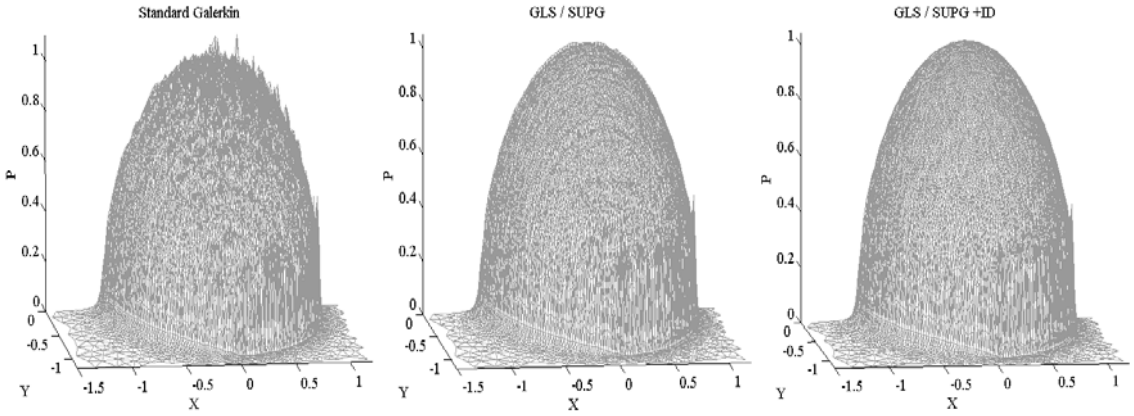

Figure 10: Stabilization effects on circular EHD contacts lubricated with a non-Newtonian lubricant (F=1000 N, p_h=1.66 GPa, α^*=18.53 GPa^{-1}, u_1= u_2=1 m/s, R=12.7 mm, T= T_0 =T_R=40 °C)

The stabilized formulations will not be reminded in this section, these are the same as described in section 2. Again, it is clear that a standard Galerkin formulation leads to an oscillatory behaviour of the solution. Applying GLS or SUPG formulations reduces the amplitude of these oscillations without completely smoothing them out. And finally, adding the ID terms to the GLS or SUPG formulations completely smoothes out the remaining oscillations.

3.1.2 Global numerical procedure

The same numerical procedure as described in section 2 is employed with only a few slight differences. At every Newton resolution, the integral terms in the generalized Reynolds equation are computed using the solution of the previous resolution. Thus an iterative linearization process is established as shown in the flow diagram of Figure 11. This iterative process is repeated until the convergence of the solution is obtained i.e. in this case, until the maximum absolute difference between the pressure solutions at two consecutive resolutions falls below 10^{-3}. The initial values for the pressure profile P and the elastic deflection profile U correspond to those of a dry / Hertzian contact or a suitable previously stored solution. As for the initial value of τ_e, it is obtained by assuming the lubricant is Newtonian and using the initial values of P, U and H_0.

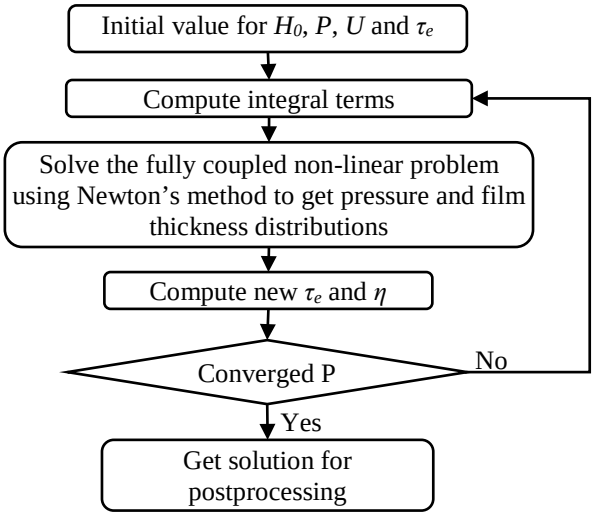

Figure 11: flow diagram for the numerical modelling of an isothermal EHL circular contact lubricated with a non-Newtonian lubricant

It is clear that the global numerical procedure requires more computational efforts than the one for the Newtonian approach and consequently, more cpu time is required. This is due to, first the calculation of the integral terms that is required at every iteration of the global procedure and second, the inconsistent linearization of the formulation for these terms (the contribution of the integral terms to the Jacobian matrix is omitted). In fact, this inconsistent linearization process leads to an additional loop in the general procedure which requires in its turn 10 to 20 iterations. Roughly speaking, for a typical case, the calculations may take between 10 to 20 minutes on a personal computer with a 2 GHz processor.

3.2 Thermal effects

In this section, the temperature throughout the lubricant film is not considered constant anymore. In fact, two heat sources lead to the global increase of temperature: the compressibility of the lubricant and frictional shear. Hence, not only the viscosity of the lubricant varies in the film thickness, but also its density. Thus a new generalized Reynolds equation that takes into account these variations is introduced by Yang and Wen [31]. The latter can be written in the following dimensionless form:

$$\nabla\cdot\left(\varepsilon''\,\nabla P\right)-\frac{\partial\left(\overline{\rho}^{*}H\right)}{\partial X}=0 \qquad (29)$$

$$\varepsilon'' = \left(\frac{\bar{\rho}}{\bar{\eta}}\right)_e \frac{H^3}{\lambda''} \qquad \left(\frac{\bar{\rho}}{\bar{\eta}}\right)_e = \frac{\bar{\eta}_e \bar{\rho}'_e}{\bar{\eta}'_e} - \bar{\rho}''_e \qquad \lambda'' = \frac{u_m R^2 \mu_R}{a^3 p_h}$$

$$\bar{\rho}^* = \frac{\left[\bar{\rho}'_e \bar{\eta}_e (u_2 - u_1) + \bar{\rho}_e u_1\right]}{u_m} \qquad \bar{\rho}_e = \int_0^1 \bar{\rho}\, dZ$$

Where:

$$\bar{\rho}'_e = \int_0^1 \bar{\rho} \int_0^Z \frac{dZ'}{\bar{\eta}} dZ \qquad \bar{\rho}''_e = \int_0^1 \rho \int_0^Z \frac{Z' dZ'}{\bar{\eta}} dZ$$

$$\frac{1}{\bar{\eta}_e} = \int_0^1 \frac{dZ}{\bar{\eta}} \qquad \frac{1}{\bar{\eta}'_e} = \int_0^1 \frac{Z\, dZ}{\bar{\eta}}$$

Equation (29) is the most general form of Reynolds equation. It is valid for both Newtonian and non-Newtonian lubricants (for a Newtonian lubricant the generalized Newtonian viscosity η is replaced by the Newtonian one μ). It takes into account the variations of both viscosity and density across the film thickness. In fact, the changes in density are due to temperature variations across the lubricant film whereas the changes in viscosity stem from both temperature and (when a generalized Newtonian lubricant is considered) shear rate variations across the film. Moreover, both density and viscosity are allowed to vary with pressure and temperature throughout the contact domain according to the relationships presented in Appendix A. Note that if the temperature in the lubricant film is assumed to be constant and equal to the ambient temperature ($T = T_0 = cst$) equation (29) reduces to the generalized Reynolds equation (26), and furthermore, if the generalized Newtonian viscosity η is replaced by the Newtonian one μ, this equation reduces to the classical Reynolds equation (1). Finally, let $\rho_0 = \bar{\rho}(P, T = T_0)$ be the two dimensional function defined on the contact domain Ω_c and describing the density variations over the latter with respect to pressure considering a constant temperature $T = T_0$. Equation (29) can be written in the following form:

$$\begin{aligned} R''(P) &= -\nabla \cdot (\varepsilon'' \nabla P) + \frac{\partial\left[\rho_0 \left(\frac{\bar{\rho}^*}{\rho_0}\right) H\right]}{\partial X} = 0 \\ &= -\nabla \cdot (\varepsilon'' \nabla P) + \left(\frac{\bar{\rho}^*}{\rho_0}\right) H \frac{\partial \rho_0}{\partial P} \frac{\partial P}{\partial X} + \rho_0 \frac{\partial\left[\left(\frac{\bar{\rho}^*}{\rho_0}\right) H\right]}{\partial X} = 0 \end{aligned} \tag{30}$$

Let: $\beta''_X = \left(\frac{\bar{\rho}^*}{\rho_0}\right) H \frac{\partial \rho_0}{\partial P}$, $\beta''_Y = 0$ and $Q'' = -\rho_0 \frac{\partial\left[\left(\frac{\bar{\rho}^*}{\rho_0}\right) H\right]}{\partial X}$

Then eq. (30) becomes:

$$R''(P) = -\nabla \cdot (\varepsilon'' \nabla P) + \beta'' \cdot \nabla P - Q'' = 0 \tag{31}$$

Hence, the generalized Reynolds equation with thermal effects also has the form of a classical Diffusion-Convection equation (applied to P) with a source term Q''. The thermal model for temperature variations in the lubricant film and the contacting elements will not be described here since this is not the main topic of this paper but all the details can be found in a previous work of the authors [6]. The latter is based on the resolution of the 3D energy equation in the lubricant film and the solid bodies.

3.2.1 Finite element procedure

The system of EHL equations formed by the generalized Reynolds equation with thermal effects, the linear elasticity equations and the load balance equation is solved using a similar Newton-Raphson approach as described in section 2. The finite element formulations for this system are not reminded here. Those are similar to the ones provided in section 2 since the generalized Reynolds equation with thermal effects also has the form of a convection / diffusion equation. The free boundary problem is treated by applying the penalty method and for heavy loads, the solution of the generalized Reynolds equation with thermal effects exhibits similar instability features as described previously. The same stabilization techniques are used to avoid them (based on a convection / diffusion form of Reynolds equation). This can be seen in Figure 12 where a test case with the same lubricant and operating conditions as in the previous section is carried out. Only this time, temperature is no longer considered as a constant throughout the lubricant film and solid bodies.

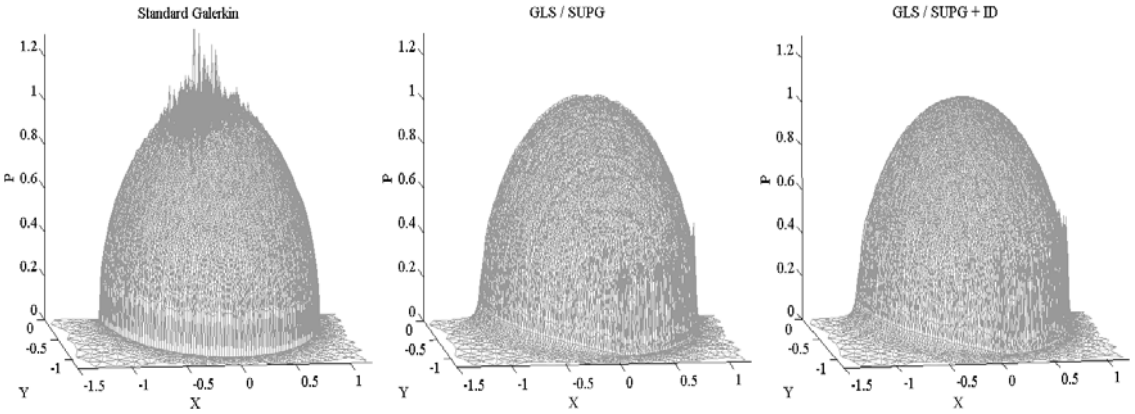

Figure 12: Stabilization effects on circular thermal EHD contacts (F=1000 N, p_h=1.66 GPa, α^*=18.53 GPa^{-1}, $u_1 = u_2$=1 m/s, R=12.7 mm)

The stabilized formulations will not be reminded in this section, these are the same as provided in section 2. Again, it is clear that a standard Galerkin formulation leads to an oscillatory behaviour of the solution. Applying GLS or SUPG formulations reduces the amplitude of these oscillations without completely smoothing them out. And finally, adding the ID terms to the GLS or SUPG formulations completely smoothes out the remaining oscillations.

3.2.2 Global numerical procedure

The global numerical procedure for thermal EHL (TEHL) modelling is much more complex than for the isothermal case. The starting point consists in defining initial values for P, U, H_0, T and τ_e. The initial values for the pressure profile P and the elastic deflection profile U correspond to those of a dry / Hertzian contact or a suitable previously stored solution. As for the initial value of τ_e, it is obtained by assuming the lubricant is Newtonian

and using the initial values of P, U, T and H_0. The initial temperature field is taken to be constant and equal to the ambient temperature T_0 throughout the contacting solids and the lubricant film.

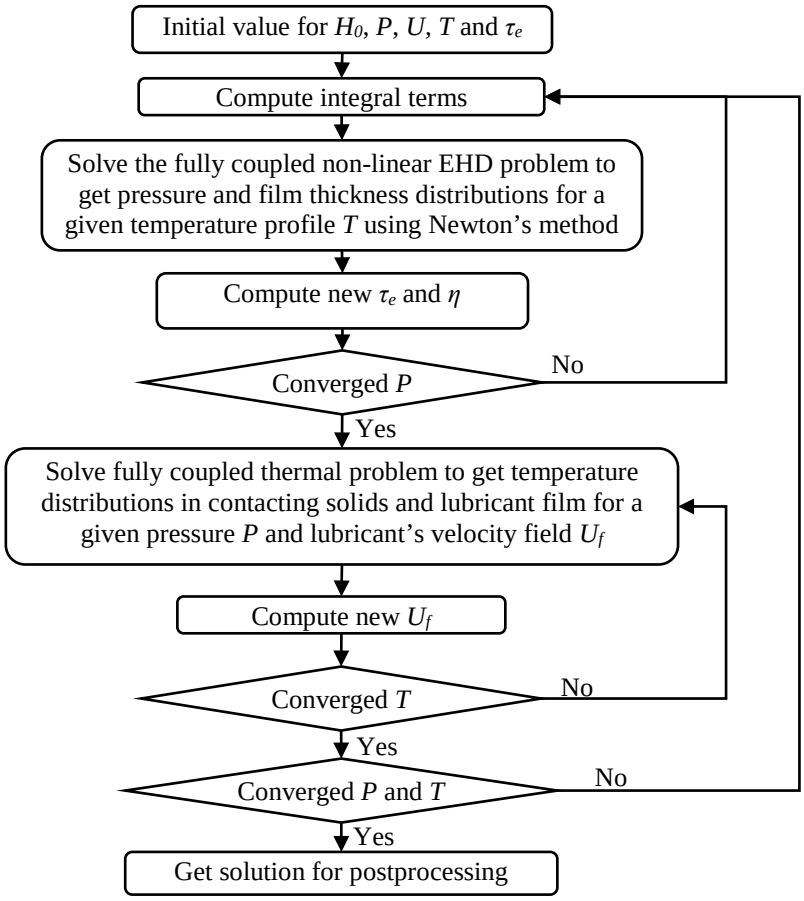

Figure 13: Flow diagram of the thermal EHL (TEHL) model

After the initial values of the different variables are defined, the system formed by the generalized Reynolds equation with thermal effects, the linear elasticity and the load balance equations is solved using a Newton-Raphson procedure. At every Newton resolution, the integral terms in the generalized Reynolds' equation with thermal effects are computed using the solution of the previous resolution. Thus an iterative procedure is introduced. It is repeated until the convergence of the solution is obtained i.e. in this case, until the maximum absolute difference between the pressure solutions at two consecutive resolutions falls below 10^{-3}.

Then the system formed by the energy equations of the contacting elements and the lubricant film is solved for a given pressure profile P and lubricant's velocity field $\vec{U}_f$. The latter is computed for a given viscosity distribution obtained using the last pressure and temperature solutions. The new temperature distribution is used to compute the new value of the lubricant's velocity field. The latter is again injected in the energy equations for a new resolution. This is repeated until the convergence of the temperature solution is obtained i.e. in this case, until the maximum relative difference between the temperature solutions at two consecutive iterations falls below 10^{-3}.

Finally, since the temperature solution is obtained for a given pressure distribution and vice versa, a final test is realized to check that the effects of the variations of any of the two

solutions on the other one has become negligible i.e. to ensure the convergence of the global algorithm with respect to the coupling procedure. The same convergence criteria as listed above are employed.

The global numerical procedure is described in the flow chart of Figure 13. More computational efforts and consequently cpu time are required than for an isothermal approach. In fact, in addition to the complementary operations that are required in the isothermal non-Newtonian case, the solution of the thermal part comes as an additional computational task. Hence, for a typical case, the calculations may take "roughly" between 30 to 60 minutes on a personal computer with a 2 GHz processor.

N.B.: The additional computational tasks required for the non-Newtonian and thermal cases are common features that are required in any EHL solver regardless of the employed approach. Hence, these cannot be considered as a drawback of the current model. In addition, since the core solver (i.e. Newton-Raphson part) of the current model has been proven to be more efficient than the state of the art existing ones (See section 2), the current EHL solver remains more efficient even in the non-Newtonian and thermal cases.

4 Conclusion

In this work, the authors introduced stabilized finite element formulations for elastohydrodynamic lubrication problems considering a Newtonian or non-Newtonian lubricant under isothermal or thermal regimes. In all cases, these formulations are based on "artificial diffusion" techniques such as SUPG, GLS or ID which are applied to the different Reynolds equations manipulated to have the form of a classical Diffusion-Convection equation with a source term. It is shown that in the one-dimensional case of Reynolds equation (i.e.: line contacts) the SUPG or GLS formulations are sufficient to remove the spurious behaviour of the solution which occurs at heavy loads when convection becomes dominant. However, for the two-dimensional case (i.e.: circular contacts), additional ID terms are required to completely smooth out the oscillations. Fortunately, although these additional terms are not residual based, they are shown to have a negligible effect on the solution.

Acknowledgments

The authors thank Prof. E. Ioannides (SKF Group Product Technical Director) for his kind permission to publish this work. They also wish to express their gratitude to the French Ministry of National Education and Scientific Research for partially financing this study.

Appendix A: density and viscosity variations with pressure, temperature and shear stress

A.1- Density variations with pressure and temperature

In this section the models used in this work for describing the density dependence on both pressure and temperature are described. The *R* index stands for the value of the corresponding parameter at a reference state (p_R, T_R) :

A.1.1- Dowson & Higginson

The mathematical expression of the Dowson & Higginson [22] model for density variations with pressure and temperature is given by:

$$\rho(p,T)=\rho_R\left[1+\frac{0.6\times10^{-9}\,p}{1+1.7\times10^{-9}\,p}-\beta_{DH}\left(T-T_R\right)\right]$$

A.1.2- Tait-equation of state

The Tait [30] equation of state is written for the volume V relative to the volume at ambient pressure V_0. The density data is obtained by simply inverting it:

$$\frac{V}{V_0}=1-\frac{1}{1+K_0^{'}}\ln\left[1+\frac{p}{K_0}\left(1+K_0^{'}\right)\right]$$

The initial bulk modulus K_0 and the initial pressure rate of change of bulk modulus K_0' are assumed to vary with temperature according to:

$$K_0=K_{0R}\exp\left(-\beta_K T\right)\quad\text{and}\quad K_0'=K_{0R}'\exp(\beta_K' T)$$

The volume at ambient pressure V_0 relative to the ambient pressure volume V_R at the reference temperature T_R is assumed to depend on temperature according to:

$$\frac{V_0}{V_R}=1+a_V\left(T-T_R\right)$$

The density relationship to pressure and temperature can be deduced from the previous equations by a simple manipulation:

$$\rho(p,T)=\rho_R\left(\frac{V_R}{V}\right)=\rho_R\left(\frac{V_R}{V_0}\times\frac{V_0}{V}\right)=\rho_R\left(\frac{1}{V_0/V_R}\times\frac{1}{V/V_0}\right)$$

A.2- Viscosity variations

In this section the models used in this work for describing the viscosity dependence on pressure and temperature are described. Moreover, if the lubricant is non-Newtonian, the shear stress dependence is also provided:

A.2.1- Pressure and temperature dependence

When the considered lubricant has a Newtonian behaviour (i.e.: the generalized Newtonian viscosity is equal to the Newtonian one $\eta=\mu$), its viscosity only depends on pressure and temperature.

A.2.1.1- WLF

The mathematical expression of the WLF [23] model describing the dependence of viscosity on both pressure and temperature is given by:

$$\mu(p,T) = \mu_g \times 10^{\frac{-C_1 \cdot (T - T_g(p)) \cdot F(p)}{C_2 + (T - T_g(p)) \cdot F(p)}}$$

$$\text{with:} \quad T_g(p) = T_g(0) + A_1 \ln(1 + A_2 p)$$
$$F(p) = 1 - B_1 \ln(1 + B_2 p)$$

A_1, A_2, B_1, B_2, C_1 and C_2 are constants characterizing each fluid and μ_g is the viscosity at the glass transition temperature T_g. The function $T_g(p)$ represents the variation of the glass transition temperature with respect to pressure based on experimental data whereas $F(p)$ represents the variation of the thermal expansion coefficient with pressure.

A.2.1.2- Roelands

The mathematical expression of the Roelands [25] model describing the dependence of viscosity on both pressure and temperature is given by:

$$\mu(p,T) = \mu_R \exp\left\{ \left(\ln(\mu_R) + 9.67 \right) \left[-1 + \left(1 + 5.1 \times 10^{-9} p \right)^{Z_0} \left(\frac{T - 138}{T_R - 138} \right)^{-S_0} \right] \right\}$$

$$\text{Where:} \quad Z_0 = \frac{\alpha}{\left[5.1 \times 10^{-9} \left(\ln(\mu_R) + 9.67 \right) \right]}$$
$$S_0 = \frac{\beta_{Roe} (T_R - 138)}{\ln(\mu_R) + 9.67}$$

A.2.1.3- Doolittle free volume model

The Doolittle [29] model is based on the free volume principle and is defined by the following relationship:

$$\mu(p,T) = \mu_R \exp\left[BR_0 \left(\frac{\frac{V_\infty}{V_{\infty R}}}{\frac{V}{V_R} - R_0 \frac{V_\infty}{V_{\infty R}}} - \frac{1}{1 - R_0} \right) \right]$$

The relative occupied volume with respect to the reference state is given by the following relationship:

$$\frac{V_\infty}{V_{\infty R}} = 1 + \varepsilon_c (T - T_R)$$

B and R_0 are constants characterizing a given lubricant, whereas V / V_R is defined by a given equation of state. This model is often associated to the Tait equation of state. Together they are known as the Tait-Doolittle free volume density and viscosity model.

A.2.2- Shear stress dependence

Finally, when the lubricant is non-Newtonian, its viscosity exhibits variations with respect to shear stress. In this work, the modified version of the Carreau model provided by Bair [27] is used to describe these variations. The latter is given by the following mathematical expression:

$$\eta = \mu_2 + \frac{\mu_1 - \mu_2}{\left[1 + \left(\frac{\tau_e}{G_c}\right)^{\beta_c}\right]^{\frac{\frac{1}{n_c}-1}{\beta_c}}} \qquad \text{where} \qquad \beta_c = \exp\left[0.657 - 0.585\ln\left(n_c\right)\right]$$

Where G_c is the liquid critical shear stress. This equation is a good approximation of the classical Carreau law for values of n_c ranging from 0.3 to 0.8, which is the range of interest in EHL applications.

Appendix B: Equivalent elastic problem

In this appendix, the theory behind the equivalent elastic problem is described. This problem is introduced in order to avoid solving the elastic deflection problem twice, under the same loading conditions, on the same geometry, using the respective material properties of solids *1* and *2*. The equivalent material properties are obtained using the half space theory. The latter states that the displacement $\delta(x, y, z)$ of a point (x, y, z) produced by a concentrated point force *F* acting normally to the surface $z = 0$ at the origin (See Figure A.1) is given, according to Love [32], by:

$$\delta(x, y, z) = \frac{F}{4\pi\mu}\frac{z^2}{r^3} + \frac{(\lambda + 2\mu)F}{4\pi\mu(\lambda + \mu)}\frac{1}{r}$$

Where λ and μ are the Lamé constants and $r = \sqrt{x^2 + y^2 + z^2}$. The Lamé constants are related to Young's modulus *E* and Poisson's coefficient υ according to:

$$\lambda = \frac{E\upsilon}{(1+\upsilon)(1-2\upsilon)} \quad \text{and} \quad \mu = \frac{E}{2(1+\upsilon)}$$

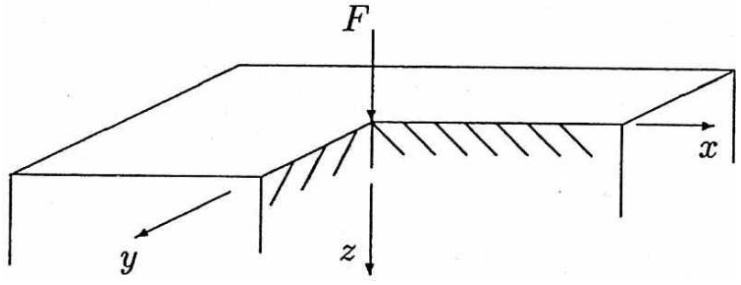

Figure B.1: Point loading of an elastic half space

Then, the equivalent displacement $\delta_{eq}(x,y,z)$ of the two solids *1* and *2* under the same concentrated point force *F* acting normally to the surface $z=0$ at the origin is given by:

$$\delta_{eq}(x,y,z)=\delta_1(x,y,z)+\delta_2(x,y,z)$$

$$\frac{F}{4\pi\mu_{eq}}\frac{z^2}{r^3}+\frac{(\lambda_{eq}+2\mu_{eq})F}{4\pi\mu_{eq}(\lambda_{eq}+\mu_{eq})}\frac{1}{r}=\frac{F}{4\pi\mu_1}\frac{z^2}{r^3}+\frac{(\lambda_1+2\mu_1)F}{4\pi\mu_1(\lambda_1+\mu_1)}\frac{1}{r}+\frac{F}{4\pi\mu_2}\frac{z^2}{r^3}+\frac{(\lambda_2+2\mu_2)F}{4\pi\mu_2(\lambda_2+\mu_2)}\frac{1}{r}$$

After simplification, the previous equation becomes:

$$\frac{1}{\mu_{eq}}\left[\frac{z^2}{r^2}+2(1-\upsilon_{eq})\right]=\frac{1}{\mu_1}\left[\frac{z^2}{r^2}+2(1-\upsilon_1)\right]+\frac{1}{\mu_2}\left[\frac{z^2}{r^2}+2(1-\upsilon_2)\right] \tag{B.1}$$

Any couple of material properties (μ_{eq},υ_{eq}) that satisfies the previous equation can be used to define the equivalent elastic problem. Here, we consider the particular case where:

$$\frac{1}{\mu_{eq}}=\frac{1}{\mu_1}+\frac{1}{\mu_2} \tag{B.2}$$

$$\Rightarrow\frac{1+\upsilon_{eq}}{E_{eq}}=\frac{1+\upsilon_1}{E_1}+\frac{1+\upsilon_2}{E_2} \tag{B.3}$$

Equation (B.1) becomes after simplification and replacing $1/\mu_{eq}$ by its expression given in (B.2) and the Lamé constant μ by its expression as a function of *E* and υ:

$$\frac{1-\upsilon_{eq}^2}{E_{eq}}=\frac{1-\upsilon_1^2}{E_1}+\frac{1-\upsilon_2^2}{E_2} \tag{B.4}$$

Thus, solving the system of equations formed by (B.3) and (B.4), one gets the equivalent material properties E_{eq} and υ_{eq}:

$$E_{eq}=\frac{E_1^2E_2(1+\upsilon_2)^2+E_2^2E_1(1+\upsilon_1)^2}{\left[E_1(1+\upsilon_2)+E_2(1+\upsilon_1)\right]^2}\quad\text{and}\quad\upsilon_{eq}=\frac{E_1\upsilon_2(1+\upsilon_2)+E_2\upsilon_1(1+\upsilon_1)}{E_1(1+\upsilon_2)+E_2(1+\upsilon_1)}$$

In order to validate the equivalent problem's theory, a test case is carried out with a dry glass-on-steel circular contact with a Hertzian pressure distribution applied in the contact region.

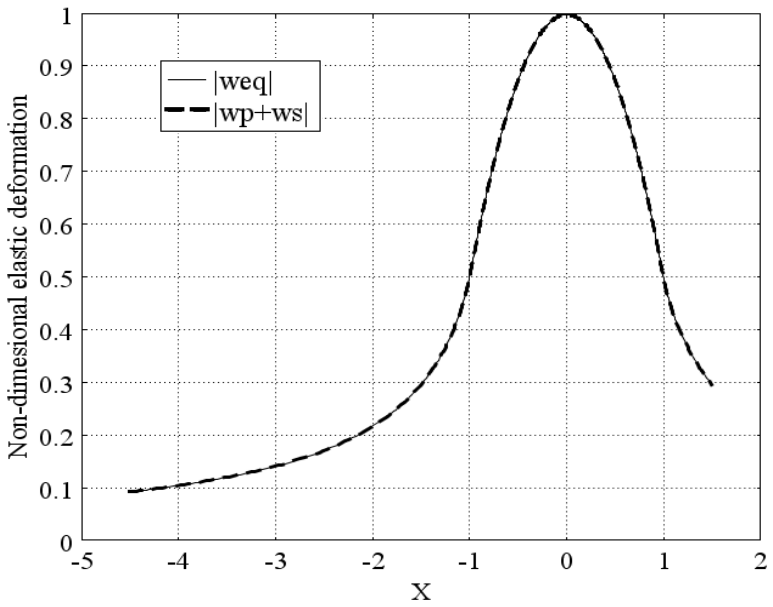

Figure B.2: Total elastic deflection of a dry glass-on-steel circular contact

Figure B.2 shows the non-dimensional elastic deflection curves on the central line in the *X*-direction obtained by both the equivalent problem defined in this section and the sum of the elastic displacements of the two contacting elements. It is clear that the two curves show a perfect match, revealing thus the equivalence between the two approaches.

Dimensionless parameters:

$$H = \frac{hR}{a^2} \qquad X = \frac{x}{a} \qquad Y = \frac{y}{a} \qquad Z = \begin{cases} z/a & \text{in the solid bodies} \\ z/h & \text{in the lubricant film} \end{cases}$$

$$\bar{\rho} = \frac{\rho}{\rho_R} \qquad \bar{\mu} = \frac{\mu}{\mu_R} \qquad \bar{\eta} = \frac{\eta}{\mu_R} \qquad P = \frac{p}{p_h}$$

Where: $\quad E' = \dfrac{2}{\dfrac{1-\upsilon_1^2}{E_1} + \dfrac{1-\upsilon_2^2}{E_2}} \qquad a = \sqrt[3]{\dfrac{3FR}{2E'}} \qquad p_h = \dfrac{3F}{2\pi a^2}$

References

[1] Oh KP and Rohde SM. Numerical Solution of the Point Contact Problem Using the Finite Element Method. *International Journal for Numerical Methods in Engineering* 1977; **11**: 1507-1518.

[2] Holmes MJA, Evans HP, Hughes TG and Snidle RW. Transient Elastohydrodynamic Point Contact Analysis Using a New Coupled Differential Deflexion Method. Part 1: Theory and Validation. *Proceedings of the Institution of Mechanical Engineers Journal of Engineering Tribology* 2003; **217 (J)**: 289-303.

[3] Lubrecht AA, Ten Napel WE and Bosma R. Multigrid, An Alternative Method for Calculating Film Thickness and Pressure Profiles in Elastohydrodynamically Lubricated Line Contacts. *ASME Journal of Tribology* 1986; **108 (4)**: 551-558.

[4] Venner CH. Multilevel Solution of the EHL Line and Point Contact Problems. *PhD Thesis* 1991, University of Twente, Encchede, The Netherlands.

[5] Habchi W, Eyheramendy D, Vergne P and Morales-Espejel, G. A Full-System Approach of the Elastohydrodynamic Line / Point Contact Problem. *ASME Journal of Tribology* 2008; **130 (2)**, DOI: 10.1115/1.2842246.

[6] Habchi W, Eyheramendy D, Bair S, Vergne P and Morales-Espejel G. Thermal Elastohydrodynamic Lubrication of Point Contacts Using a Newtonian / Generalized Newtonian Lubricant. *Tribology Letters* 2008; **30 (1)**: 41-52.

[7] Hertz H. Uber die Berührung fester Elastischer Körper. *Journal fur die reine und angewandte Mathematik* 1882; **92**: 156-171.

[8] Reynolds O. On the Theory of the Lubrication and its Application to Mr Beauchamp Tower's Experiments, Including an Experimental Determination of the Viscosity of Olive Oil. *Philosophical Transactions of the Royal Society of London* 1886; **177**: 157-234.

[9] Wu SR. A Penalty Formulation and Numerical Approximation of the Reynolds-Hertz Problem of Elastohydrodynamic Lubrication. *International Journal of Engineering Science* 1986; **24 (6)**: 1001-1013.

[10] Dowson D and Higginson GR. A Numerical Solution of the Elastohydrodynamic Problem. *Journal of Mechanical Engineering Science* 1959; **1 (1)**: 6-15.

[11] Evans HP and Snidle RW. The Isothermal Elastohydrodynamic Lubrication of Spheres. *ASME Journal of Lubrication Technology* 1981; **103**: 547-557.

[12] Hamrock BJ and Dowson D. Isothermal Elastohydrodynamic Lubrication of Contacts, Part I – Theoretical Formulation. *ASME Journal of Lubrication Technology* 1976; **98 (2)**: 223-229.

[13] Lubrecht AA. The Numerical Solution of the Elastohydrodynamically Lubricated Line and Point Contact Problem Using Multigrid Techniques. *PhD Thesis* 1987, University of Twente, Enschede, The Netherlands.

[14] Hughes TG, Elcoate CD and Evans HP. A Novel Method for Integrating First- and Second-Order Differential Equations in Elastohydrodynamic Lubrication for the Solution of Smooth Isothermal, Line Contact Problems. *International Journal of Numerical Methods in Engineering* 1999; **44**: 1099-1113.

[15] Brooks AN and Hughes TJR. Streamline-Upwind/Petrov-Galerkin Formulations for Convective Dominated Flows with Particular Emphasis on the Incompressible Navier-Stokes Equations. *Computer Methods in Applied Mechanics and Engineering* 1982; **32**:199- 259.

[16] Galeão AC, Almeida RC, Malta SMC and Loula AFD. Finite Element Analysis of Convection Dominated Reaction-Diffusion Problems. *Applied Numerical Mathematics* 2004; **48**: 205-222.

[17] Hughes TJR, Franca LP and Hulbert GM. A New Finite Element Formulation for Computational Fluid Dynamics: VII. The Galerkin-Least-Squares Method for Advective-Diffusive Equations. *Computer Methods in Applied Mechanics and Engineering* 1989; **73**: 173-189.

[18] Hughes TJR. Multiscale Phenomena: Green's Functions, the Dirichlet-to-Neumann Formulation, Subgrid Scale Models, Bubbles and the Origins of Stabilized Methods. *Computer Methods in Applied Mechanics and Engineering* 1995; **127**: 387-401.

[19] Oñate E. Derivation of Stabilized Equations for Numerical Solution of Advective-Diffusive Transport and Fluid Flow Problems. *Computer Methods in Applied Mechanics and Engineering* 1998; **151**: 233-265.

[20] Johnson C, Nävert U and Pitkäranta J. Finite Element Methods for Linear Hyperbolic Problems. *Computer Methods in Applied Mechanics and Engineering* 1984; **45**: 285-312.

[21] Johnson C and Pitkäranta J. An Analysis of the Discontinuous Galerkin Method for a Scalar Hyperbolic Equation. *Mathematics of Computation* 1986; **46**: 1-26.
[22] Dowson D and Higginson GR. Elastohydrodynamic Lubrication. The Fundamental of Roller and Gear Lubrication. *Oxford, Pergamon*, 1966.
[23] Yasutomi S, Bair S and Winer WO. An Application of a Free-Volume Model to Lubricant Rheology, (1) Dependence of Viscosity on Temperature and Pressure. *ASME Journal of Tribology* 1984; **106**: 291-312.
[24] Zienkiewicz OC and Taylor RL. The Finite Element Method, Volume 3, Fluid Dynamics, 5th edition. *Butterworth & Heinmann*, England, 2000.
[25] Roelands CJA. Correlational Aspects of the Viscosity-Temperature-Pressure Relationship of Lubricating Oils. *PhD thesis* 1966, Technische Hogeschool Delft, The Netherlands.
[26] Venner CH and Lubrecht AA. Multilevel Methods in Lubrication. *Tribology Series (37), Elsevier*, Amsterdam, 2000.
[27] Bair S. A Rough Shear-Thinning Correction for EHD Film Thickness. *STLE Tribology Transactions* 2004; **47**: 361-365.
[28] Najji B, Bou-Said B and Berthe D. New Formulation for Lubrication with Non-Newtonian Fluids. *ASME Journal of Tribology* 1989; **111**: 29-33.
[29] Doolittle AK. Studies in Newtonian Flow II, The Dependence of the Viscosity of Liquids on Free-Space. *Journal of Applied Physics* 1951; **22:** 1471-1475.
[30] Hogenboom DL, Webb W and Dixon JD. Viscosity of Several Liquid Hydrocarbons as a Function of Temperature, Pressure and Free Volume. *Journal of Chemical Physics* 1967; **46 (7)**: 2586-2598.
[31] Yang P and Wen S. A Generalized Reynolds Equation for Non-Newtonian Thermal Elastohydrodynamic Lubrication. *ASME Journal of Tribology* 1990; **112**: 631-636.
[32] Love A. E. H. – A treatise on the Mathematical Theory of Elasticity, 4th edition. *Dover*, New York, 1944.